

Rotationally Induced Transitions in Atomic Collisions

A. Russek

The University of Connecticut, Storrs, Connecticut 06268

(Received 21 June 1971)

Excitation effects due to rotational motion of the internuclear line during an atomic collision are considered in the two-state approximation. These effects are governed by a pair of first-order differential equations which couple adiabatic levels of different angular momentum (e.g., σ to π transitions), which actually do cross. The equations are cast in such a form that the solution for rotational excitation may be expressed in terms of the well-known Landau-Zener solution. It is found, however, that application of these results to a real collision suffers from defects which are worse for the case of rotational excitation than for ordinary Landau-Zener transitions. The coupled differential equations are then solved numerically to document the shortcomings of the Landau-Zener approach to a real collision and to present cross-section results which are free from these defects.

I. INTRODUCTION

Since 1932, excitation effects in near-adiabatic atomic collisions have been treated in terms of a two-state approximation which describes the dynamic coupling between two adiabatic molecular levels at a pseudocrossing. This has come to be known as the "Landau-Zener approximation."¹⁻³ A convenient summary of the model may be found in the quantum-mechanics text of Landau and Lifshitz.⁴ Use of this model was, however, restricted to excitation effects due to the radial component of the relative motion only. Bates⁵⁻⁷ realized that the adiabatic molecular states used in representing the transient molecule are quantized along the body-fixed internuclear axis. Since the internuclear line is rotating during the collision process, he recognized a second dynamic coupling mechanism between the adiabatic molecular levels. This coupling mechanism is called "rotational coupling" and will be used, in Sec. II, to extend the Landau-Zener model to take into account all terms in the Hamiltonian which cause departure from adiabaticity in the two-level approximation. It should be mentioned here that Lichten⁸ also treats rotational coupling, but from a different (albeit equivalent) point of view. A comparison of the two approaches will be presented at the end of Sec. II.

Despite the fact that rotational coupling in the two-state approximation can be solved by the same mathematical techniques as those used in standard Landau-Zener transitions, some problems still remain. These problems are treated in Sec. III and have to do with the breakdown in the validity of the Landau-Zener approximation when applied to a real collision. The principal defects are found to lie in the rather substantial interval around the crossing in which the Landau-Zener transition takes place. Bates⁹ considered this effect for transitions due to radial motion (i. e., standard Landau-Zener transitions). It is here shown that the defect is even

worse when considering rotational transitions, mainly because rotational excitation occurs predominantly at impact parameters close to the crossing radius, where the angular velocity at the crossing is greatest. This creates several difficulties all at once. (i) The transition regions for the two traversals of the level crossing made by the collision trajectory strongly overlap, and (ii) the energy difference at the crossing cannot be considered to vary linearly along the trajectory in the region of strong interaction between the two levels. Because of these difficulties, the pair of coupled differential equations is solved numerically in Sec. III for the case of rotational transitions. Cross sections are presented for rotational excitation in the approximation in which the collision trajectories are taken to be undeviated straight lines.

II. ROTATIONAL EXCITATION

A. Derivation of Excitation Probability in Landau-Zener Approximation

In this section we will first review the general interaction between two adiabatic states, in order to display more clearly the comparison between the Landau-Zener transition and rotational excitation.

Let \vec{R} stand for the vector internuclear separation and \vec{r} stand for the coordinates of all electrons of the colliding systems in a space-fixed frame. In addition, let \vec{r}' stand for these same electron coordinates in a body-fixed frame. The distinction between the two frames is needed in discussing rotational excitation. For convenience, the z' axis is taken to be the internuclear axis of the quasimolecule. Finally, let H stand for the electronic Hamiltonian. The adiabatic states $\psi_1(\vec{r}', \vec{R})$ and $\psi_2(\vec{r}', \vec{R})$ are defined as eigenstates of the electronic Hamiltonian H for fixed internuclear separation \vec{R} ,

$$H \psi_i(\vec{r}', \vec{R}) = \epsilon_i(R) \psi_i(\vec{r}', \vec{R}), \quad i = 1, 2. \quad (1)$$

The variables \vec{r}' are used here because the elec-

tronic states are quantized in the body-fixed frame. For example, a π state has azimuthal quantum number $\Lambda = 1$ about the internuclear axis.

In the two-state approximation, the state Ψ describing the quasimolecule during the collision process can be written, in the impact parameter formulation, as

$$\Psi = c_1(t) \psi_1(\vec{r}', \vec{R}) \exp[-(i/\hbar) \int^t \epsilon_1 d\tau] + c_2(t) \psi_2(\vec{r}', \vec{R}) \exp[-(i/\hbar) \int^t \epsilon_2 d\tau], \quad (2)$$

where, it must be remembered, \vec{R} is a function of time which defines the collision trajectory of the nuclei. In this paper, the trajectory will be taken as a straight-line path.

Everything is determined in the state (2) by the solutions of the eigenvalue equations (1) except for the coefficients c_1 and c_2 . These are determined by Schrödinger's time-dependent equation

$$\left(H - i\hbar \frac{\partial}{\partial t} \right) \Psi = 0, \quad (3)$$

which the true state satisfies. Within the context of the two-state approximation, however, (3) is replaced by the weaker condition

$$\langle \psi_1 | H - i\hbar \frac{\partial}{\partial t} | \Psi \rangle = 0, \quad \langle \psi_2 | H - i\hbar \frac{\partial}{\partial t} | \Psi \rangle = 0, \quad (4)$$

where the inner product is taken over electronic coordinates only. Remembering that ψ_1 and ψ_2 are dependent on time because they are functions of \vec{R} , Eqs. (4) yield, with the help of Eq. (1),

$$\begin{aligned} [\dot{c}_1 + c_1 \langle \psi_1 | \dot{\psi}_1 \rangle] \exp[-(i/\hbar) \int^t \epsilon_1 d\tau] \\ + c_2 \langle \psi_1 | \dot{\psi}_2 \rangle \exp[-(i/\hbar) \int^t \epsilon_2 d\tau] = 0, \\ [\dot{c}_2 + c_2 \langle \psi_2 | \dot{\psi}_2 \rangle] \exp[-(i/\hbar) \int^t \epsilon_2 d\tau] \\ + c_1 \langle \psi_2 | \dot{\psi}_1 \rangle \exp[-(i/\hbar) \int^t \epsilon_1 d\tau] = 0. \end{aligned} \quad (5)$$

When carrying out the differentiations of the wave functions with respect to time, it must be kept in mind that the electronic coordinates are defined with respect to the body-fixed internuclear axis, which is rotating during the collision. As a consequence,⁵⁻⁷

$$\dot{\psi}_i = \dot{R} \frac{\partial \psi_i}{\partial R} + i \frac{\dot{\Theta}}{\hbar} L_{\perp} \psi_i, \quad (6)$$

where \dot{R} is the relative radial velocity of the two nuclei, $\dot{\Theta}$ is the angular velocity of the internuclear axis, and L_{\perp} is that component of the electronic angular momentum operator, in the body-fixed frame, which is perpendicular to the plane of the collision trajectory.

The first term in (6) is responsible for the conventional Landau-Zener transitions. Inasmuch as $\partial \psi_i / \partial R$ has the same electronic symmetry proper-

ties as ψ_i , the Landau-Zener transitions couple only states of identical symmetry (e.g., σ_g -to- σ_g transitions). On the other hand, the second term in (6) is responsible for rotational excitation; it couples, for example, σ and π states, but does not couple σ -to- σ or π -to- π transitions. To see this, take the collision plane to be the X - Z plane in the space-fixed frame and Z' the internuclear axis in the body-fixed frame. Then L_{\perp} is the y' component (recall that it is in the body-fixed frame) and can be written in the form

$$L_{\perp} = L_{y'} = [(L_{x'} + iL_{y'}) - (L_{x'} - iL_{y'})]/2i = (L_+ - L_-)/2i, \quad (7)$$

where L_+ and L_- denote the raising and lowering operators for azimuthal angular momentum along the internuclear axis.

From Eq. (7) it is clear that the second term in (6) couples σ states to π states and vice versa. It also couples π to δ states, etc.; but it will not couple two states having the same z' component of angular momentum. Thus, when discussing rotational excitation, the symmetry of the two states must be different, with the consequence that

$$\left\langle \psi_i \left| \frac{\partial}{\partial R} \right| \psi_j \right\rangle = \left\langle \psi_j \left| \frac{\partial}{\partial R} \right| \psi_i \right\rangle = 0, \quad (8)$$

and the first term on the right-hand side of (6) will not contribute. Also, because the states ψ_i are normalized,

$$\langle \psi_i | \dot{\psi}_i \rangle = \frac{1}{2} \frac{\partial}{\partial t} \langle \psi_i | \psi_i \rangle = \frac{1}{2} \frac{\partial}{\partial t} 1 = 0. \quad (9)$$

[Note that the result (9) assumes that ψ_i is real or has at most a complex factor such as $\exp(i\phi')$ which does not vary with time. Such is the case for molecular orbitals.] With the help of Eqs. (8) and (9), Eqs. (5) reduce to

$$\dot{c}_1 + i \frac{\dot{\Theta}}{\hbar} c_2 \langle \psi_1 | L_{\perp} | \psi_2 \rangle \exp[-i \frac{\dot{\Theta}}{\hbar} \int^t (\epsilon_2 - \epsilon_1) d\tau] = 0, \quad (10)$$

$$\dot{c}_2 + i \frac{\dot{\Theta}}{\hbar} c_1 \langle \psi_2 | L_{\perp} | \psi_1 \rangle \exp[-i \frac{\dot{\Theta}}{\hbar} \int^t (\epsilon_1 - \epsilon_2) d\tau] = 0.$$

In the neighborhood of a level crossing at $R = R_x$, the energy difference $\epsilon_2 - \epsilon_1$ can be considered to vary linearly with internuclear separation and, therefore, linearly with time as well:

$$(\epsilon_2 - \epsilon_1)/\hbar = b(R - R_x) = \alpha t, \quad (11a)$$

with

$$\alpha = \frac{v_R}{\hbar} \frac{d}{dR} (\epsilon_2 - \epsilon_1) \Big|_{R=R_x}. \quad (11b)$$

Also, the matrix element in (10) can be considered to remain essentially constant in the region of strong interaction between the levels:

$$V = \langle \psi_1 | L_1 | \psi_2 \rangle. \quad (12)$$

Note that V has the dimensions of angular momentum, because Θ has been extracted. The quantities α and V are taken to be constants. With these substitutions, Eqs. (10) become

$$\begin{aligned} \dot{c}_1 + i\omega V \hbar^{-1} c_2 \exp[-i \hbar^{-1} \int^t (\epsilon_2 - \epsilon_1) d\tau] &= 0, \\ \dot{c}_2 + i\omega V^* \hbar^{-1} c_1 \exp[+i \hbar^{-1} \int^t (\epsilon_2 - \epsilon_1) d\tau] &= 0, \end{aligned} \quad (13)$$

with ω and v_R being the angular and radial relative velocities at the level crossing. If a straight-line trajectory with impact parameter ρ is taken, ω and v_R are given by

$$\begin{aligned} \omega &= v_{\perp}/R_x = v\rho/R_x^2, \\ v_R &= v(R_x^2 - \rho^2)^{1/2}/R_x. \end{aligned} \quad (14)$$

Now Eqs. (13) are exactly in the mathematical form as those solved by Zener,² with only two minor differences. (i) The constant ωV in (13) replaces the constant coupling matrix element in Zener's work. (ii) The present paper uses a time dependence $\exp(-i \hbar^{-1} \int^t \epsilon d\tau)$ which is now standard, whereas Zener used the alternative formulation in which the Schrödinger equation $H\psi = -i \hbar \dot{\psi}$ so that the time dependence comes out as $\exp(+i \hbar^{-1} \int^t \epsilon d\tau)$. This, of course, makes no difference in the physical results.

One important difference must, however, be noted. The adiabatic states of identical symmetry considered by Zener do not actually cross. Zener therefore introduced what Lichten¹⁰ has since termed the "diabatic" states, which do cross. On the other hand, the adiabatic states used in the present paper are of different symmetry and do, in fact, cross. Thus, the results of Zener can be taken over intact.

The solutions obtained by Zener to the Eqs. (13) do not actually yield workable expressions for the coefficients at all time t , only at $t = \pm \infty$. The coefficients are expressed in terms of Weber functions of complex argument, which are not tabulated, but the asymptotic behavior of which are known. Thus, Zener demonstrated that for initial conditions

$$|c_1(-\infty)| = 0, \quad |c_2(-\infty)| = 1, \quad (15)$$

the final values are given by

$$\begin{aligned} |c_1(+\infty)|^2 &= 1 - e^{-2\pi\gamma}, \\ |c_2(+\infty)|^2 &= e^{-2\pi\gamma}, \end{aligned} \quad (16)$$

where, with the constants as they appear in Eqs. (13),

$$\gamma = \frac{\omega^2 |V|^2}{\hbar(d/dt)(\epsilon_2 - \epsilon_1)|_{t=0}} = \frac{\omega^2 |V|^2}{\hbar v_R(d/dR)(\epsilon_2 - \epsilon_1)|_{R=R_x}}. \quad (17)$$

Finally, ω and v_R may be expressed in terms of the initial relative velocity v and impact parameter ρ :

$$\gamma = \frac{v |V|^2}{\hbar(d/dR)(\epsilon_2 - \epsilon_1)|_{R=R_x}} \frac{\rho^2}{R_x^3 (R_x^2 - \rho^2)^{1/2}}. \quad (18)$$

It will be noted that for rotational excitation, γ varies linearly with relative velocity. By contrast, γ varies inversely with relative velocity in the standard Landau-Zener excitation.

To summarize the results just obtained, the probability p for making a rotational transition at a level crossing between two adiabatic states differing by one unit of azimuthal angular momentum is

$$p = 1 - e^{-2\pi\gamma}, \quad (19)$$

with γ given by Eq. (18).

B. Comparison with Lichten Approach

Although the basic physics in this section and in the work of Lichten are equivalent, they appear sufficiently dissimilar at first glance that a word of explanation is in order. Lichten uses the rotational coupling term of Bates in defining the adiabatic molecular state. He is therefore quantizing in a rotating frame of reference. As a consequence, the only nonadiabatic interaction term which remains is that due to the radial component of motion, and Lichten is then able to apply the standard Landau-Zener results to complete the calculation. On the other hand, the formulation of the present paper remains in the space-fixed frame and uses the Bates rotational term as a dynamic interaction between the two adiabatic states defined in the space-fixed frame.

Clearly, the reference frame used to describe a process cannot have any physical consequence. However, there can be important mathematical differences as to which aspects can be dealt with more readily. Thus, in his formulation, Lichten finds it easy to encompass excitation with arbitrary change in azimuthal angular momentum. Calculations in the present paper, on the other hand, are restricted to unit change in this angular momentum. To handle here the sort of excitations which Lichten can easily consider would require inclusion of virtual excitations to intermediate states and thereby immediately destroy all the simplifications inherent in the two-state approximation.

On the other hand, the formulation used in this paper has compensating benefits. It permits easy inclusion of nonadiabatic effects due to the variation in angular velocity of the rotating internuclear line. This aspect is considered in Sec. III, along with other effects which cause a breakdown in the validity of the Landau-Zener approach to a real collision.

III. APPLICATION TO COLLISIONS

In applying the results of Sec. II to a real collision, it must be remembered that the crossing radius R_x if crossed at all will be crossed twice, once on the way in and once on the way out. Thus the probability ϕ for making a transition as a result of the collision is generally considered to be

$$\phi = 2p(1-p), \quad (20)$$

which is a sum of $p(1-p) + (1-p)p$, each of which represents the probability of making a transition on one of the crossings but not on the other. It is recognized, in accepting (20), that the probabilities for each of the two alternative ways of achieving the transition should not, in fact, be added. Rather, the amplitudes should be added and then the square of the absolute value obtained. This will have the result of producing oscillations about the values given by Eq. (20) as any of the relevant parameters is varied. Such oscillations can, in selected cases, actually be seen, but are generally averaged over by the experimental technique.

Such a simple picture of the collision process is, unfortunately, not generally valid unless the crossing radius R_x is large compared to a relevant parameter to be discussed below. It will be recalled that the assumptions made in Sec. II, in deriving the probability for rotational excitation at a level crossing, are, in the region of significant interaction between the two states, the following: (i) The relative radial and angular velocities, v_R and ω , and the matrix element V governing the interaction can all be considered to remain essentially constant; and (ii) the energy separation between the two levels varies linearly with time. For a wide variety of collisions, however, this is not the case. The probability p given by Eq. (19), it will be remembered, is derived from the asymptotic behavior of the Weber function. Consideration must be given to the time (or distance) interval required before asymptotic conditions obtain. Bates has shown that the interval of internuclear separation ΔR on either side of the crossing radius R_x in which the probabilities of two states achieve the major portion of their changes from initial to final values is given by

$$\Delta R = (\pi \hbar v_R s/b)^{1/2}, \quad (21)$$

where $\hbar b$, defined in Eq. (11a), is the slope of the energy difference at the level crossing and s is a number of the order of, but greater than, unity. This is illustrated in Fig. 1 by a direct numerical integration of Eqs. (13) to exhibit the probabilities as functions of internuclear separation in the vicinity of a single crossing. Clearly, if the turning point R_0 of the nuclear trajectory lies within an interval ΔR of the crossing radius, the simple picture

of two separate traversals of the crossing radius breaks down. If

$$R_x - R_0 \leq (\pi \hbar v_R s/b)^{1/2},$$

Eq. (20) is invalid, and if

$$R_x - R_0 \gg (\pi \hbar v_R s/b)^{1/2},$$

Eq. (20) is valid (if phase interference oscillations are averaged over).

The breakdown in the validity of Eq. (20) is particularly bad in the case of rotational excitation. From Eqs. (18) and (19) it will be seen that γ is large and p approximately unity when the impact parameter is closest to the crossing radius. Indeed, a significant amount of excitation can occur for impact parameters greater than R_x . Moreover, since the contribution of larger impact parameters is more heavily weighted in the total cross section, it is clear that the Landau-Zener approach described above is inadequate except for cases in which $R_x \gg \Delta R$.

To better understand the rotational excitation process, therefore, Eqs. (13) were solved numerically. The most convenient independent variable for the purpose is Θ , the orientation angle of the internuclear axis:

$$\frac{dc_i}{dt} = \dot{\Theta} \frac{dc_i}{d\Theta} = \omega \frac{dc_i}{d\Theta}, \quad (22)$$

$$\int^t (\epsilon_2 - \epsilon_1) d\tau = \int^\Theta [(\epsilon_2 - \epsilon_1)/\omega] d\Theta,$$

where, it must be remembered, ω is not a con-

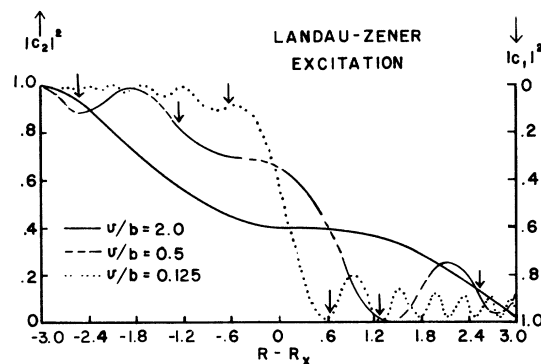


FIG. 1. Nonrotational Landau-Zener transitions. The three curves show the values of $|c_2|^2$ and $|c_1|^2$ as functions of $R - R_x$ for the three velocities $v/b = 0.125, 0.5,$ and 2.0 . In all three cases, the matrix elements have been so chosen that $2\pi\gamma = 3.14$. Thus, the asymptotic value of $|c_2|^2$ for each curve will be $e^{-3.14} = 0.043$. The ordinate scale on the left-hand side of the figure gives $|c_2|^2$, while that on the right-hand side gives $|c_1|^2$. The vertical arrows touching each curve show ΔR computed from Eq. (21) with s taken equal to unity. This choice should yield a somewhat small value for ΔR , precisely what the results show.

stant, but a function of Θ . With this substitution, Eqs. (13), after dividing through by ω , take the form

$$\frac{dc_1}{d\Theta} + iV\hbar^{-1}c_2 e^{-i\zeta(\Theta)} = 0, \quad (23a)$$

$$\frac{dc_2}{d\Theta} + iV^*\hbar^{-1}c_1 e^{+i\zeta(\Theta)} = 0, \quad (23b)$$

with

$$\zeta(\Theta) = \frac{1}{\hbar} \int^{\Theta} \frac{\epsilon_2(\Theta) - \epsilon_1(\Theta)}{\omega(\Theta)} d\Theta. \quad (24)$$

For a straight-line path and with energy separation varying linearly with internuclear separation as in (11a),

$$\zeta(\Theta) = \frac{b\rho}{\hbar v} \int^{\Theta} \left(\frac{\rho}{\cos\Theta} - R_x \right) \frac{d\Theta}{\cos^2\Theta}. \quad (25)$$

As shown in Fig. 2, the angle Θ is measured with respect to \vec{R}_0 and varies from $-\frac{1}{2}\pi$ to $+\frac{1}{2}\pi$, which are the only singular points. The equations were therefore integrated over the domain $-1.35 \leq \Theta \leq +1.35$ rad which also served as the lower limit of the integral in (25).

Figures 3 and 4 illustrate typical results for the variation of $|c_2|^2$ and $|c_1|^2$ with Θ as the collision progresses. It will be remembered that the final transition probability $\varphi = |c_1(+\frac{1}{2}\pi)|^2$. In all cases the curve crossing has been taken at $R_x = 1$ a.u. and the coupling matrix taken to be $V = 0.6$ a.u. Figure 3 shows the variation for several values of incident velocity but for fixed impact parameter. Contrary to what would be expected on the basis of the simple two-independent-crossings picture, the results show that the main change in probability occurs in the region between the two level crossings. (Here, these are marked by the vertical arrows.) There is no indication of a rapid variation in probability centered about each level crossing, with rather constant probability elsewhere. The reason for the behavior seen in Fig. 3 is not hard to find; it lies in the phase development $\zeta(\Theta)$ given by Eq. (24). When ζ changes rapidly (i. e., when $|d\zeta/d\Theta|$

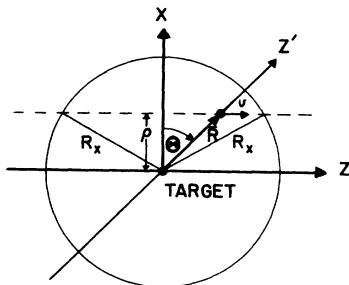


FIG. 2. Collision geometry in the laboratory frame.

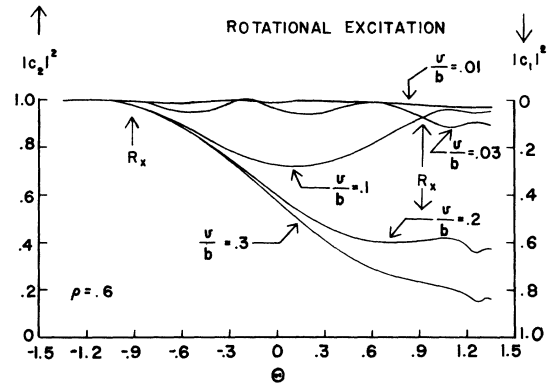


FIG. 3. Rotational excitation. The ordinate at the left gives $|c_2|^2$; the ordinate at the right gives $|c_1|^2$. The abscissa gives internuclear orientation, Θ . Curves are shown for several values of incident velocity, but with identical value of impact parameter $\rho = 0.6$, crossing radius $R_x = 1.0$, and matrix element $V = 0.6$ (all in a.u.). The level crossing points are indicated by the vertical arrows marked R_x . The values of $|c_1|^2$ for the largest value of Θ shown are, for all practical purposes, φ .

large), integration of Eqs. (23) yields c_1 and c_2 to be almost constants, performing rapid oscillations of negligible amplitudes about these constant values. Conversely, when $|d\zeta/d\Theta|$ is small, c_1 and c_2 make large changes. From (24),

$$\left| \frac{d\zeta}{d\Theta} \right| = \frac{|\epsilon_2(\Theta) - \epsilon_1(\Theta)|}{\hbar\omega(\Theta)}, \quad (26)$$

where, it will be recalled, the geometry has been so chosen that $\omega \geq 0$. Now, going from a crossing outward, the absolute value of the energy difference monotonically increases while ω in the de-

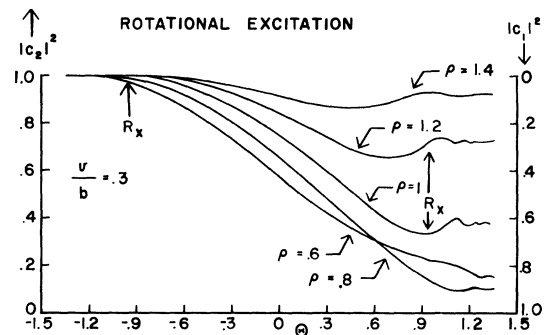


FIG. 4. Rotational excitation. The ordinate at the left gives $|c_2|^2$; the ordinate at the right gives $|c_1|^2$. The abscissa gives internuclear orientation, Θ . Curves are shown for several values of impact parameter ρ , but with identical values of incident velocity $v/b = 0.3$, crossing radius $R_x = 1.0$, and matrix element $V = 0.6$ (all in a.u.). The level crossing points are indicated by the vertical arrows marked R_x . The values of $|c_1|^2$ for the largest value of Θ shown are, for practical purposes, φ .

TABLE I. The first column shows the velocity divided by slope of the energy difference at the crossing, in atomic units, while the second column shows the total phase change between the two crossings. The crossing radius and impact parameter are 1.0 and 0.6 a.u., respectively.

v/b	$\Delta\zeta = \zeta(-\Theta_x) - \zeta(+\Theta_x)$	R_x	Θ_x	ρ
0.01	$6.44 \times 2\pi$	1.0	53.3°	0.6
0.03	$2.15 \times 2\pi$	1.0	53.3°	0.6
0.10	$0.64 \times 2\pi$	1.0	53.3°	0.6
0.20	$0.32 \times 2\pi$	1.0	53.3°	0.6
0.30	$0.22 \times 2\pi$	1.0	53.3°	0.6

nominator monotonically decreases; both behaviors work in the same direction to make the ratio increase very rapidly going outward from a level crossing. On the other hand, going *inward* from a crossing (i.e., in the region between the two level crossings), the absolute value of the energy difference again increases, but here ω also increases and the ratio remains rather constant over the entire region between the two crossings. This can be most clearly seen in the case $v/b = 0.03$; the oscillations are nearly sinusoidal in Θ . It is also true in all other cases depicted in Fig. 3, but it is not so obvious. In the three cases $v/b = 0.1, 0.2,$ and 0.3 , ζ does not change by a full 2π in the entire intercrossing region; for $v/b = 0.01$ the oscillations are too small to be drawn clearly. Table I shows the total change in ζ between the two crossings for the five cases of Fig. 3. The first column shows the velocity divided by slope of the energy difference at the crossing, in atomic units, while the second column shows the total phase change between the two crossings. The crossing radius and impact parameter are 1.0 and 0.6 a.u., respectively. From Fig. 3 and Table I, it is seen that the transition here takes place over the entire region between the two crossings.

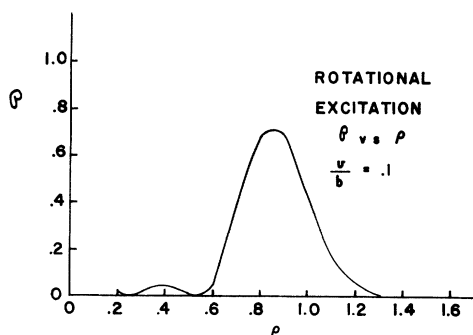


FIG. 5. Rotational excitation probability versus impact parameter. The curve shows ϕ vs ρ for $v/b = 0.1$ and $V = 0.6$, in a.u.

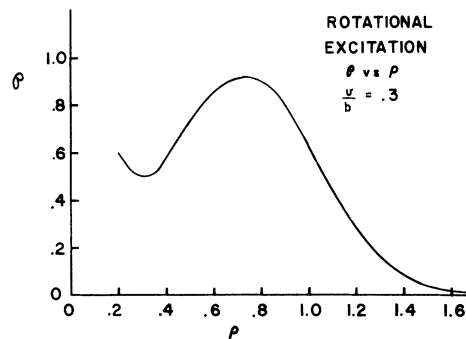


FIG. 6. Rotational excitation probability versus impact parameter. The curve shows ϕ vs ρ for $v/b = 0.3$ and $V = 0.6$, in a.u.

Figure 4 shows the functions $|c_1(\Theta)|^2$ and $|c_2(\Theta)|^2$ for fixed value of $v/b = 0.3$, but for several values of impact parameter. From this figure it is seen that ϕ achieves its maximum value at an impact parameter somewhat less than the crossing radius. (Note that ϕ should be read from the scale at the right in Figs. 3 and 4.) ϕ is quite large at $\rho = R_x$ and does not drop off to negligible values until ρ is substantially larger than R_x . This behavior is illustrated more clearly in Figs. 5 and 6 which show ϕ as a function of ρ . Smaller values of v/b yield a ϕ which is sharply peaked at a value just under R_x . Larger values of v/b yield a broad-peaked ϕ which has its peak at somewhat lower values and extends further out beyond $\rho = R_x$. Since the curves in Figs. 5 and 6 must be multiplied by $2\pi\rho$ before integrating to obtain the cross section, it is clear that impact parameters greater than $\rho = R_x$ make a major contribution to the total cross section for rotational excitation. In Figs. 5 and 6, no results are shown for impact parameters less than $\rho = 0.2$. The reason for this is that as $\rho \rightarrow 0$, ω approaches the δ

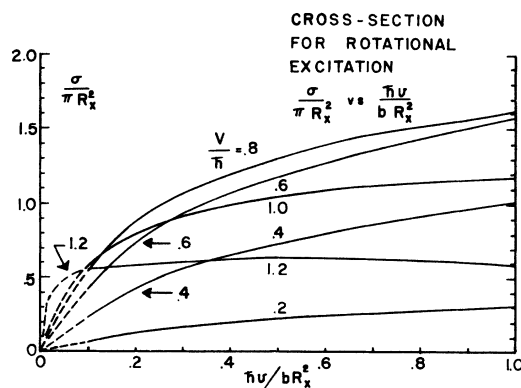


FIG. 7. Collision cross section for rotational excitation. The reduced total cross section $\sigma_{\text{rot}}/\pi R_x^2$ for rotational excitation is plotted as functions of reduced velocity $\hbar v/bR_x^2$ for collisions with several values of angular momentum coupling V , given in a.u.

function, $\omega(\Theta) \rightarrow \pi\delta(\Theta)$. In this limit all levels are strongly coupled and the near-adiabatic behavior inherent in the two-level approximation completely breaks down (see Schneiderman and Russek).¹¹ Thus, any results for $\rho < 0.2$ would be completely spurious. Fortunately, such small impact parameters make a negligible contribution to the total cross section for rotational excitation.

Finally, Fig. 7 shows the total cross section for rotational excitation as a function of incident velocity for the straight-line trajectories used in this paper. Five physical parameters appear in Eqs. (23)–(25): V , b , R_x , v , and ρ . Since the impact parameter is integrated over in obtaining a total cross section σ , this would normally be expected to depend on four variables. Three of these are properties of the projectile plus target molecular system: V , b , and R_x . The fourth is the incident velocity v . However, because of the form of Eqs. (23) and the straight-line approximation for ζ , Eq. (25), the results in Fig. 7 can be expressed in terms of only two variables, with the help of scaling parameters. If the dimensionless quantities

$$x = \rho/R_x, \quad y = \tilde{n}v/bR_x^2 \quad (27)$$

are defined, then $2\pi\rho d\rho = 2\pi R_x^2 x dx$, and the cross section can be written in the form

$$\sigma_{\text{rot}} = \pi R_x^2 \int_0^\infty \phi(x, y, V) 2x dx. \quad (28)$$

The quantity πR_x^2 is the geometric cross section for getting inside the crossing radius. It will be remembered that in the two-independent-crossing picture, ϕ is always $\leq \frac{1}{2}$,

$$\sigma \leq \frac{1}{2} \pi R_x^2 \quad (29)$$

in the two-independent-crossing picture. A glance at Fig. 7 shows that this is far from the case for rotational excitation.

ACKNOWLEDGMENT

The computational part of this paper was carried out in the Computer Center of the University of Connecticut, which is supported in part by grant No. GJ-9 of the National Science Foundation.

¹L. Landau, *Physik. Z. Sowjetunion* **2**, 46 (1932).
²C. Zener, *Proc. Roy. Soc. (London)* **A137**, 696 (1932).
³E. C. G. Stückelberg, *Helv. Phys. Acta* **5**, 369 (1932).
⁴L. D. Landau and E. M. Lifshitz, *Quantum Mechanics*, translated by J. B. Sykes and J. S. Bell (Addison-Wesley, Reading, Mass., 1965), Sec. 87.
⁵D. R. Bates, *Proc. Roy. Soc. (London)* **A240**, 437 (1957).
⁶D. R. Bates, *Proc. Roy. Soc. (London)* **A243**, 15

(1957).
⁷D. R. Bates, *Proc. Roy. Soc. (London)* **A245**, 299 (1958).
⁸W. Lichten, *Phys. Rev. A* (to be published).
⁹D. R. Bates, *Proc. Roy. Soc. (London)* **A257**, 22 (1960).
¹⁰W. Lichten, *Phys. Rev.* **131**, 229 (1963).
¹¹S. B. Schneiderman and A. Russek, *Phys. Rev.* **181**, 311 (1969).

Rearrangement-Channel Operator Approach to Models for Three-Body Reactions. I

Michael Baer*† and Donald Kouri

Department of Chemistry, University of Houston, Houston, Texas 77004

(Received 21 December 1970)

The channel operators $\tau_{\gamma\alpha}$ describing scattering from configuration α to configuration γ are utilized in considering a model for three-body rearrangement scattering. The $\tau_{\gamma\alpha}$ are those defined by $V_\alpha + V_\gamma(E - H + i\epsilon)^{-1} V_\alpha$. Two well-known forms of integral equations for the $\tau_{\gamma\alpha}$ obtained from this expression are explicitly solved for the model potential surface. Using these explicit solutions, results are examined in the limit that no dissociative continuum is present. It is found that the integral equations in which the $\tau_{\gamma\alpha}$ are not explicitly coupled do not yield the correct results for this limiting case. Integral equations explicitly coupling the $\tau_{\gamma\alpha}$ give limiting results in agreement with those obtained by more-common boundary-matching techniques. These results indicate that the major effects of the dissociative continuum may be accounted for by considering the coupled equations for the $\tau_{\gamma\alpha}$ (at least so long as one is well below threshold for the production of three free particles).

I. INTRODUCTION

The formal theory of rearrangement collisions

has been the subject of many investigations which have resulted in a large number of alternative approaches to reactions.¹ These various approaches